

---

# Interpretable Deep Clustering

---

Jonathan Svirsky, Ofir Lindenbaum  
Faculty of Engineering  
Bar-Ilan University  
{svirskj,ofir.lindenbaum}@biu.ac.il

## Abstract

Clustering is a fundamental learning task widely used as a first step in data analysis. For example, biologists often use cluster assignments to analyze genome sequences, medical records, or images. Since downstream analysis is typically performed at the cluster level, practitioners seek reliable and interpretable clustering models. We propose a new deep-learning framework that predicts interpretable cluster assignments at the instance and cluster levels. First, we present a self-supervised procedure to identify a subset of informative features from each data point. Then, we design a model that predicts cluster assignments and a gate matrix that leads to cluster-level feature selection. We show that the proposed method can reliably predict cluster assignments using synthetic and real data. Furthermore, we verify that our model leads to interpretable results at a sample and cluster level.

## 1 Introduction

Clustering is an essential task in data science that enables researchers to discover and analyze latent structures in complex data. By grouping related data points into clusters, researchers can gain insights into the underlying characteristics of the data and identify relationships between samples and variables. Clustering is used in various scientific fields, including biology [24, 18, 5], physics [16, 22, 3], and social sciences [32]. For example, in biology, clustering can identify different disease subtypes based on molecular or genetic data. In psychology, based on survey data, clustering can identify different types of behavior or personality traits.

One of the most common applications of clustering in bio-medicine is the analysis of gene expression data, where clustering can be used to identify groups of genes with similar expression patterns across different samples. Scientists are often interested in clustering the high-dimensional points corresponding to individual cells, ideally recovering known cell populations while discovering new and perhaps rare cell types. Bio-med gene expression data is generally represented in tabular high-dimensional format, thus making it difficult to obtain accurate clusters with meaningful structures. In addition, interpretability is a crucial requirement for real-world bio-med datasets where it is vital to understand the biological meaning behind the identified clusters. While there are existing works on interpretability methods such as kernel PCA-based variables transformation proposed in [25], and a bunch of deep non-interpretable clustering models such as [29, 14, 4, 23] which are more powerful and flexible than kernel methods. Our goal in this work is to design a novel deep clustering model with built-in interpretability functionality. In addition, we propose an architecture that could also be applied to biomedical tabular data.

This work presents Interpretable Deep Clustering (IDC), an unsupervised two-stage clustering method that first selects samples-specific informative features, enabling reliable data reconstruction. Then uses the sparsified data to learn the cluster assignments by optimizing neural network parameters subject to a clustering objective function. In addition, the method provides both instance-level and cluster-level explanations represented by the selected feature set. The model learns instance-level *local gates* that select a subset of features during autoencoder training sufficient to reconstruct the

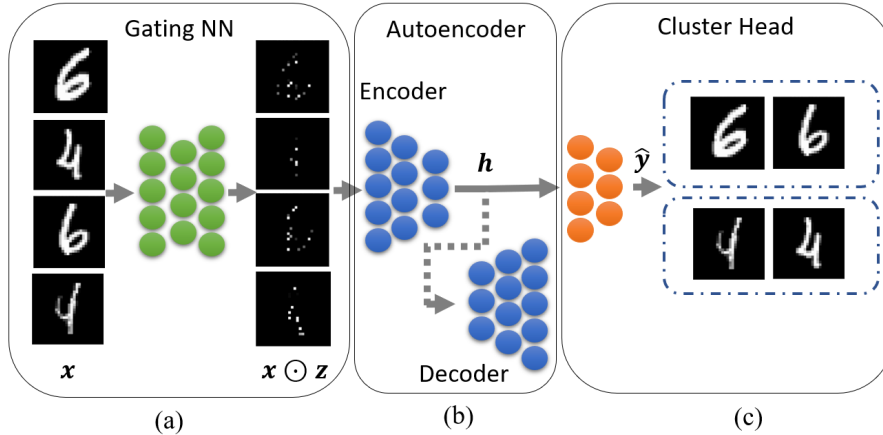


Figure 1: Illustration of the proposed model. During the first stage of training, we optimize only the parameters of Gating Network (green) and Autoencoder (blue) that reconstructs  $\hat{x}$  from latent embedding  $h$ . The gating Network learns sparse gates  $z$  from input sample  $x$  such that  $x \odot z$  is sufficient in terms of the reconstruction task of Autoencoder. During the second stage, the Clustering head (orange) is optimized to predict cluster assignments  $\hat{y}$  from the latent embedding  $h$  by minimizing the mean cluster coding rate.

original sample. The *global gates* for cluster-level interpretability are derived from the cluster label assignments learned by the model. To enforce sample-level interpretations, the gates are encouraged by the recently proposed discrimination constraint denoted as the total coding rate. In the following sections, we provide a detailed description of our approach.

## 2 Related Work

**Unsupervised Feature Selection** The problem of unsupervised feature selection involves identifying variables useful for downstream tasks such as data clustering. Towards this goal, Sokar et al. [30] proposed a sparse training procedure for the autoencoder model to select global gates for a given dataset through drop-and-grow optimization. However, the method was not verified on the clustering task, which is more challenging and requires more accurate features under unsupervised training. [19, 28] removes nuisance features using a graph Laplacian-based score. The method is verified by training  $K$ -means clustering on the selected global gates for each dataset. Both methods lack local interpretations - what features are unique for each sample in a cluster. In [13], the authors apply self-supervision to train masked autoencoder during the unsupervised pretraining step, but the features are selected during supervised training in the second step. Our setup is fully unsupervised in terms of both gates and cluster learning. While there are recent works on supervised local feature selection [35, 34], we are not aware of any local unsupervised feature selection schemes.

**Interpretable clustering** [8] is a pioneering work for applying unsupervised feature selection and clustering. The work proposes a probabilistic model that performs feature selection by using beta-Bernoulli prior in the context of a Dirichlet process mixture for clustering. While the method selects cluster-level and dataset-level features, our method provides interpretability for sample-level granularity. In [6], the authors proposed tree-based  $k$ -Means clustering of a dataset. While the whole tree structure serves as an explanation, one has to define the number of features chosen by the method. In addition, the explanations are static for a given dataset and rely on the whole set of features. Our method learns local gates for each sample in the dataset by optimizing the neural network as a gate selector and produces sample-level interpretations.

**Deep clustering** Recently, several methods were proposed for NN-based clustering, to name a few: [7, 23, 14, 27, 4, 21, 29, 26]. However, the primary domain of these works is vision, and they do not apply to tabular datasets. We introduce a NN model intended for high dimensional datasets such as bio-med data and is also interpretable. [14] introduced total coding rate loss that is adopted by our model and is based on maximum coding rate reduction (MCR<sup>2</sup>) [36]. One of the essential requirements in [14] is designing a dataset-specific augmentation used in an additional constraint term during the training, such as cosine similarity between latent embeddings of an original and augmented sample version. While such augmentations could be easily designed for the visual domain, the tabular domain becomes more challenging for this scheme. In our work, we propose to learn the

sparse representation of a sample to retain essential feature variables for clustering. In addition, we apply Total Coding Rate loss [14] to select diverse features instead of constraining the latent space with this objective.

### 3 Problem Setup

We are interested in clustering data points  $\{\mathbf{x}_i, y_i\}_{i=1}^N$ , where  $\mathbf{x}_i \in \mathbb{R}^D$  are  $D$ -dimensional vector-valued observations of general type, i.e., tabular that do not obey a particular feature structure. Our goal is to learn an interpretable clustering model defined by the tuple  $\langle f_\Theta, \mathcal{S}^g \rangle$  such that  $f_\Theta(x_i) = \{\hat{y}_i, \mathcal{S}_i^l\}$  where  $\hat{y}_i \in \{1, 2, \dots, K\}$  is an accurate clustering assignment, and  $\mathcal{S}_i^l$  is a local feature importance set for sample  $i$  and defined by  $\mathcal{S}_i^l = \{s_i^j : s_i^j \in [0, 1], j \in \{0, \dots, D-1\}\}$ .  $\mathcal{S}^g \in [0, 1]^{K \times D}$  is a global feature importance matrix where each gating vector of size  $D$  is learned for  $K$  clusters. By forcing  $|\mathcal{S}_k^l| \ll D$ , we can attenuate nuisance features and identify (sample-specific) subsets of informative features, thus improving the interpretability of the clustering model.

We aim to design a model that performs well in the clustering task, i.e., can identify clusters with semantically related samples. Furthermore, we want the model to be interpretable to enable important downstream analysis tasks such as marker gene identification in biological datasets [12]. We propose a novel model that performs clustering and local feature selection to achieve this goal. The model learns to exclude nuisance input features that do not contribute to the clustering learning task. In addition, local feature selection produces unique explanations for each sample which are meaningful for explainability tasks on model predictions. We use several metrics to demonstrate that our model improves interpretability while leading to accurate clustering results.

Our model is trained without access to any labeled data. In the evaluation step, we only use labels to evaluate the quality of our model in terms of feature selection and clustering by measuring the clustering Accuracy (ACC) based on ground truth categories  $y_i$  (labels).

## 4 Method

### 4.1 Intuition

We propose a two-step framework that learns sample-level gates and latent representation in the first step by self-supervised training. The model learns both *local gates* for interpretable input space representation and latent embedding to better discriminate between samples. In the second step, the learned representations are assigned into clusters. The *global gates* are learned based on the clustering assignment, which is learned by maximizing the sum of *coding rate* for each cluster. Finally, the method produces clustering assignments for each sample, local gates for sample-level interpretation, and global gates for the cluster-level explanation. In the following subsection, we present the proposed framework and architecture design.

### 4.2 Local Self Supervised Feature Selection

Given unlabeled observations  $\{\mathbf{x}_i\}_{i=1}^N$  we want to learn a prediction function  $f_\theta$  (parametrized using a NN) and sets of indicator vectors  $\mathbf{s}_i \in \{0, 1\}^D$  that will "highlight" which subset of variables the model should rely on for clustering each sample  $\mathbf{x}_i$ . This will enable the model to attain fewer features for each sample and reduce overfitting when predicting the clusters of unseen samples.

Towards this goal, we extend the recently proposed stochastic gates [19, 33] to learn the indicator vector. Stochastic gates are continuously relaxed Bernoulli variables that were demonstrated effective for many sparsity-based applications [17, 15, 10]. Each stochastic gate (for feature  $d$  and sample  $i$ ) is defined based on the following hard thresholding function

$$z_i = \max(0, \min(1, 0.5 + \boldsymbol{\mu}_i + \boldsymbol{\epsilon}_i)),$$

where  $\boldsymbol{\epsilon}_i$  is drawn from  $\mathcal{N}(0, \sigma^2)$  and  $\sigma$  is fixed throughout training and controls the injected noise, is fixed to 0.5 in our model as suggested in [33]. The sample-specific parameters  $\boldsymbol{\mu}_i \in \mathbb{R}^D, i = 1, \dots, N$  are predicted based on a *gating* network  $f_{\theta_1}$  such that  $\boldsymbol{\mu}_i = f(\mathbf{x}_i | \theta_1)$ , where  $\theta_1$  are the weights of the *gating* network. These weights are learned simultaneously with the weights of the *prediction* network

$\theta_2$  by minimizing the following loss:

$$\mathbb{E}[\mathcal{L}(f_{\theta_2} \circ f_{\theta_1}(\mathbf{x}_i \odot \mathbf{z}_i)) + \mathcal{L}_{reg}(\mathbf{z}_i)], \quad (1)$$

where  $\mathcal{L}$  is a desired prediction loss, e.g., clustering objective function or reconstruction error.  $\odot$  represents the Hadamard product (element-wise multiplication), and we compute its empirical expectation over  $\mathbf{x}_i$  and  $\mathbf{z}_i$ , for  $i$  in a batch of size  $B$ . The term  $\mathcal{L}_{reg}(\mathbf{z}_i)$  is a regularizer that is designed to sparsify the gates and is defined by

$$\mathcal{L}_{reg}(\mathbf{z}_i) = \|\mathbf{z}_i\|_0. \quad (2)$$

After taking the expectation (over  $\mathbf{z}_i$ ),  $\mathcal{L}_{reg}$  can be rewritten using a double sum in terms of the Gaussian error function (erf):

$$\mathcal{L}_{reg} = \frac{1}{N} \sum_{i=1}^N \sum_{d=1}^D \left( \frac{1}{2} - \frac{1}{2} \operatorname{erf} \left( -\frac{\mu_i^d + 0.5}{\sqrt{2}\sigma} \right) \right). \quad (3)$$

We pick autoencoder as a prediction network to select only informative features for clustering and disregard nuisance features. By training with self-supervision and multiple reconstruction losses, the network learns a latent embedding of the input sample and drives the gating network to open gates only for features required to reconstruct data. The model consists of the following:

- *Gating Network*,  $f_{\theta_1} : \mathbf{X} \rightarrow \mathbf{Z}$ , that predicts the gates  $\mathbf{z}_i \in [0, 1]^{|S|}$  based on the sample  $\mathbf{x}_i$ .
- *Encoder*,  $f_{\theta_2} : \mathbf{X} \odot \mathbf{Z} \rightarrow \mathbf{H}$ , that learns an embedding  $\mathbf{h}_i$  based on the element-wise gated sample  $\mathbf{x}_i$ .
- *Decoder*,  $f_{\theta_3} : \mathbf{H} \rightarrow \hat{\mathbf{X}}$ , that reconstructs  $\mathbf{x}_i$  based on the embedding  $\mathbf{h}_i$ .

To enforce the model to learn informative local gates, we apply input-space and latent-space augmentations. We equip the model with the following losses:

- *Input reconstruction loss*,  $\mathcal{L}_{recon}^1(f_{\theta_3} \circ f_{\theta_2}(\mathbf{x}_i), \mathbf{x}_i)$ , which measures the deviation of estimated  $\hat{\mathbf{x}}_i$  from the input sample  $\mathbf{x}_i$ .
- *Input denoising reconstruction loss*,  $\mathcal{L}_{recon}^2(f_{\theta_3} \circ f_{\theta_2}(\mathbf{x}_i \odot m_{rand}), \mathbf{x}_i)$ , where  $m_{rand} \in \{0, 1\}^D$  is a random binary mask generated for each sample  $\mathbf{x}_i$ . We generate a mask such that about 90% – 99% of the input features are multiplied by zero value, which indicates that the gate is closed. The loss pushes the method to pay less attention to unnecessary features for the reconstruction.
- *Latent denoising reconstruction loss*,  $\mathcal{L}_{recon}^3(f_{\theta_3}(\mathbf{h}_i \cdot h_{noise}), \mathbf{x}_i)$ , where  $h_{noise} \sim \mathcal{N}(1, \sigma_h)$  is a noise generated from a normal distribution with mean one and scale  $\sigma_h$  which is a dataset-specific hyperparameter. This term aims to improve latent embedding representation by small perturbation augmentation to treat small sample-size datasets.
- *Gated input reconstruction loss*,  $\mathcal{L}_{recon}^4(f_{\theta_3} \circ f_{\theta_2} \circ f_{\theta_1}(\mathbf{x}_i), \mathbf{x}_i)$ , which measures the deviation of estimated  $\hat{\mathbf{x}}_i$  from the input sample  $\mathbf{x}_i$ .  $\hat{\mathbf{x}}_i$  is obtained by applying gating network on  $\mathbf{x}_i$ . The loss is used to learn input space denoising with trainable gates rather than random masks.
- *Gates total coding loss*,  $\mathcal{L}_{gtr}(\mathbf{z}_i)$ , that encourages the model to select unique gates for each sample is defined by the equation:

$$\mathcal{L}_{gtr} = -\frac{1}{2} \cdot \log \det(\mathbf{I} + \lambda_1 \cdot \mathbf{Z}\mathbf{Z}^T), \quad (4)$$

which is approximately the negative Shannon coding rate of a multivariate Gaussian distribution [36],  $\mathbf{I}$  is the identity matrix, and  $\mathbf{Z}$  is the local gates learned so far. The loss is inspired by [14] and pushes the model to increase the amount of information represented in  $\mathbf{Z}$ .

We apply the  $\|\cdot\|_1$  norm for all reconstruction terms since it is less sensitive to outliers and may be applied to different kinds of content. The final sparse prediction loss  $\mathcal{L}_{sparse}$  is given by the next formula:

$$\mathcal{L}_{sparse} = \sum_{i=1}^4 \mathcal{L}_{recon}^i + \mathcal{L}_{gtr} + \beta_t \cdot \mathcal{L}_{reg}, \quad (5)$$

where  $\beta_t$  is increased from zero up to  $\beta_{max}$  value in cosine function schedule.

Equipped with this loss, our model sparsifies the input samples to the minimum number of features that contain the required information for the clustering step. While input denoising reconstruction loss applies a random mask during the learning, the gated input reconstruction loss allows for learning a local mask, or gates, that hides noise features and serves as interpretations later. The gates’ total coding loss encourages the covariance matrix of selected gates to be diagonal, thus providing unique gates for each sample in the dataset in expectation.

### 4.3 Cluster assignments with Global Interpretations

In the clustering phase, we aim to compress the learned representations of gated samples of  $\mathbf{X}$  into  $K$  clusters and predict cluster-level gates. We use the next sub-networks:

- *Clustering Head*,  $f_{\theta_4} : \mathbf{H} \rightarrow \hat{\mathbf{Y}}$ , which learns cluster assignments. The model outputs  $K$  logits values  $\pi_i$  for each sample which are converted to cluster assignment probabilities  $\hat{y}_i$  by Gumbel-Softmax [11] reparameterization:

$$\hat{y}_i = \frac{\exp((\log(\pi_i) + g_i)/\tau)}{\sum_{j=1}^K \exp((\log(\pi_j) + g_j)/\tau)}, \quad \text{for } i = 1, \dots, K. \quad (6)$$

where  $\{g_k\}_{k=1}^K$  are i.i.d samples drawn from Gumbel(0, 1) distribution, and  $\tau$  is a temperature hyper parameter. High values of  $\tau$  produce a uniform distribution of  $\hat{y}$  while decreasing the temperature yields one-hot vectors.

- *Global Gates Matrix*,  $\mathbf{Z}_G^{K \times D}$  where each row is an index of cluster and each column is an index of input space features. The matrix is optimized as a global feature selection model, where each cluster has its own feature set.
- *Auxiliary Classifier*,  $f_{\theta_6} : \mathbf{X} \odot \mathbf{Z} \odot \mathbf{Z}_G \rightarrow \hat{\mathbf{Y}}$ , which is trained by pseudo labels obtained by the clustering head  $f_{\theta_4}$  with cross-entropy loss.

The primary purpose of the auxiliary classifier is to train Gates Matrix as a prediction network. The locally sparse samples  $\mathbf{x}_i \odot \mathbf{z}_i$  learned with autoencoder are multiplied by global gates  $\mathbf{Z}_G$  and fed into the single-hidden-layer classifier. The classifier is trained to output the cluster assignments  $\hat{y}_i$  identical to those predicted with Cluster Head.

For the clustering head, we use the next loss:

$$\mathcal{L}_{head} = \sum_{k=1}^K \frac{1}{2} \cdot \log \det(\mathbf{I} + \lambda_2 \cdot \mathbf{H}_k \mathbf{H}_k^T), \quad (7)$$

where  $\mathbf{H}_k$  is a set of embeddings learned during the autoencoder training for cluster  $k$ . In contrast to 9, here we would like to decrease the coding rate on average for each cluster of embeddings  $\mathbf{H}_k$  to make the clusters more compact. The embeddings are not optimized during this step, and only cluster assignments are learned.

Finally, similarly to the previous step, we use regularization loss term  $\mathcal{L}_{reg}$ , which sparsifies the gates in the global gates matrix:

$$\mathcal{L}_{clust} = \mathcal{L}_{head} + \mathcal{L}_{CE} + \beta_t \cdot \mathcal{L}_{reg}. \quad (8)$$

## 5 Interpretability

The interpretability could be required for different levels of the task: one may require a unique explanation for each data sample that correlates the most with the model predictions. The second level depends on the model predictions granularity - for each symbolic group, one could ask the explanation for each group, which features are common across samples in the same group and unique between groups. While the model’s internal functionality may remain a black box to the practitioner, the correlation between the input space of feature values and model predictions sheds some light on the model’s interpretability. Several criteria were recently proposed to evaluate the interpretability of supervised models [34, 2]. We present them in the following paragraphs and discuss their modifications to our unsupervised setting.

**Uniqueness** The motivation for uniqueness is opposite to the *stability* metric proposed in [34, 2], which requires the selected features to be consistent between close samples. Instead, we propose to measure the uniqueness of the selected features for similar samples, which is more intuitive for local explanations for each sample. We define *uniqueness* of the explanations by:  $\min_{x_i, x_k \leq \epsilon} \frac{\|w_i - w_k\|_2}{\|x_i - x_k\|_2}$ , where  $w_{i,k}$  are feature set for samples  $x_{i,k}$ , and the expression should be maximized.

**Diversity** To get unique explanations for each cluster, where explaining features are different clusters, we adopt the *diversity* metric [34]. This metric could be addressed globally by measuring if the clusters are explained well. We expect a good interpretability model to identify different sets of variables as driving factors for explaining distinct clusters. The diversity is computed by negative mean Jaccard similarity between cluster-level active gates across all pairs of clusters. The model should maximize the expression:  $1 - \sum_{i \neq j} \frac{J(S_{c_i}, S_{c_j})}{K \cdot (K-1)/2}$ , where  $S_{c_i, j}$  is a set of open global gates for cluster  $c_i$ .

**Faithfulness** To evaluate the feature significance for prediction, we exploit *faithfulness* property. It is evaluated by removing features one by one (based on their importance) and calculating the correlation between the predictivity drop and the feature importance [34, 2].

## 6 Experiments

### 6.1 Implementation

We implement our model in Pytorch and run experiments on a Linux server with NVIDIA GeForce GTX 1080 Ti and Intel(R) Core(TM) i7-8700 CPU @ 3.20GHz. We share our code on Github<sup>1</sup>. Our model has two main versions: the first includes only the autoencoder and clustering head along with a learnable global gating matrix, denoted in the experiments by **IDC** (w/o gates). The second version adds a gating network to the first one, and it is the full proposed model. Every part presented in Figure 1 is trained with a separate optimizer and learning rate. The reader can find the technical details in the appendix.

### 6.2 Datasets

Table 1: The datasets used in our experiments. We include low sample size datasets along with standard deep clustering benchmarks with a large number of samples.

Dataset	Synthetic	MNIST <sub>10K</sub>	MNIST <sub>60K</sub>	FashionMNIST <sub>60K</sub>	TOX-171	ALLAML	PROSTATE	SRBCT	BIASE	INTESTINE
D	13	784	784	784	5,748	7,192	5,966	2,308	25,683	3,775
N	3,268	10,000	60,000	60,000	171	72	102	83	56	238
K	4	10	10	10	4	2	2	4	4	13

We conduct four types of experiments. First, we verify the clustering and local feature selection capabilities of our method on a synthetic dataset. Then, we verify that the sparsity constraint preserves or even improves clustering quality for two commonly used clustering benchmarks, MNIST and FashionMNIST. In the third experiment, we evaluate our method on small sample size real-world datasets with many features. Finally, we evaluate the interpretability of the model on an MNIST subset of size 10,000 samples and present the quality of the selected features. The datasets used in the experiments are summarized in Table 1. In addition, we compare the interpretability metrics measured for our method against other popular feature explanation schemes.

### 6.3 Evaluation

**Interpretability quality** To evaluate the interpretability of the proposed model, we test it on the MNIST subset of 10,000 images, 1,000 images for each class. We measure diversity, uniqueness, and faithfulness described in Section 5. The evaluation is done on subsets of  $1K$  images by taking the mean value after ten iterations. We compare the interpretability of our method to the popular Shap feature importance detection method [20] implemented here <sup>2</sup> and its alternative Gradient Shap <sup>3</sup>. In

<sup>1</sup><https://github.com/jsvir/idc>

<sup>2</sup><https://github.com/slundberg/shap>

<sup>3</sup>[https://captum.ai/api/gradient\\_shap.html](https://captum.ai/api/gradient_shap.html)

Table 2: Interpretability results. Shap top features obtained for the trained  $K$ -means model. Integrated Gradients and Gradients Shap explainers are applied on the clustering head of our model (CH). Gating network selects diverse and unique features while learned global gates come with stronger faithfulness.

Method	ACC $\uparrow$	$ S $ $\downarrow$	Uniqueness $\uparrow$	Diversity $\uparrow$	Faithfulness $\uparrow$
$K$ -Means + Shap	52.9	13	0.12	<b>98.7</b>	0.85
CH + IntegGrads	<b>82.73</b>	13	0.11	35.3	0.76
CH + GradShap	<b>82.73</b>	13	0.06	49.2	0.76
IDC local gates	<b>82.73</b>	13	<b>0.65</b>	94.8	<b>0.94</b>
IDC global gates	81.57	<b>7</b>	0.05	86.1	0.90

addition, we present the results of Integrated Gradients [31], which are trained on the IDC clustering model predictions. As a prediction model for Shap, we use  $K$ -Means.

**Clustering accuracy** We use two popular clustering metrics, Clustering Accuracy (ACC) and Normalized Mutual Information (NMI), to quantify the clustering performance. The two metrics take values in the  $[0, 1]$  range, and a higher score implies better clustering performance.

## 6.4 Results

### 6.4.1 Synthetic dataset

Table 3: Results on Synthetic dataset with three informative features and ten nuisance features. Our model is accurate and achieves the highest F1-score that measures if the model selects the correct features.

Method	ACC $\uparrow$	F1-score $\uparrow$
IDC	<b>99.91</b>	<b>88.95</b>
$K$ -Means+Shap	25.72	49.65

We verify our method first on the synthetic dataset. The dataset consists of three informative features  $\{x_i\}_1^3$  such that  $x_i \in [-1, 1]$  generated to produce isotropic Gaussian blobs with clusters standard deviation 0.5 and ten nuisance background features with values drawn from  $\mathcal{N}(0, \sigma = 0.01)$  resulting in 13 total features. We present the top features in Figure 2. The samples are equally distributed between 4 clusters, with  $\sim 800$  samples in each cluster. Given the first two dimensions  $\{x_1, x_2\}$ , only 3 clusters are separable, and the same property holds for dimensions pair  $\{x_1, x_3\}$ . We expect the interpretable clustering model to be able to select the correct support features for each cluster. In Table 3, we present the accuracy of the clustering where  $K$ -Means was run 20 times, and the F1-score was measured on the selected features. We expect clusters with purple and blue labels to be explained by features  $\{x_1, x_2\}$  and clusters with green and yellow labels by  $\{x_1, x_3\}$ . To evaluate the effectiveness of the model, we calculate both clustering accuracy (ACC) and F1-score that measures the quality feature selection. Since for each sample, we know what the informative features are, we can calculate precision and recall for gate-level feature selection. While the  $K$ -Means fails to produce accurate clustering, our method achieves 99.91% accuracy. Additionally, it has a good ability to select the relevant features. The results are presented in Table 3.

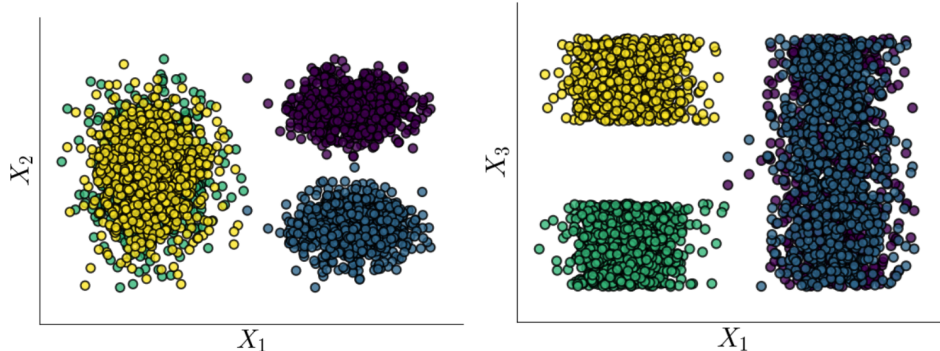


Figure 2: Visualization of Synthetic dataset. To separate between clusters, the model should select one of the pairs  $\{x_1, x_2\}$  or  $\{x_1, x_3\}$  of non-background features.

### 6.4.2 Interpretability results on MNIST<sub>10K</sub> dataset

As a baseline for interpretability, we exploit the Shap values model which is trained on the  $K$ -Means model predictions. First we train  $K$ -Means on MNIST<sub>10K</sub> dataset. Since Shap requires a set of

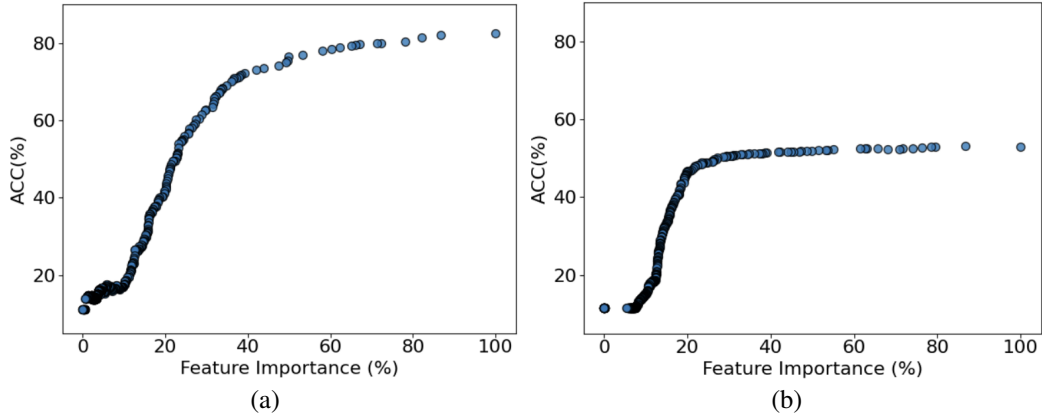


Figure 3: Faithfulness of the proposed method on MNIST<sub>10K</sub> subset. Feature importance values are obtained by the sum of active features across the subset, then sorting in ascending order and dividing by the maximal value to get importance %. Accuracy is measured each time by masking out the features. Accuracy drop and feature importance are very correlated for our approach 0.94 (a) while less correlated for Shap features for  $K$ -Means clustering 0.85 (b).

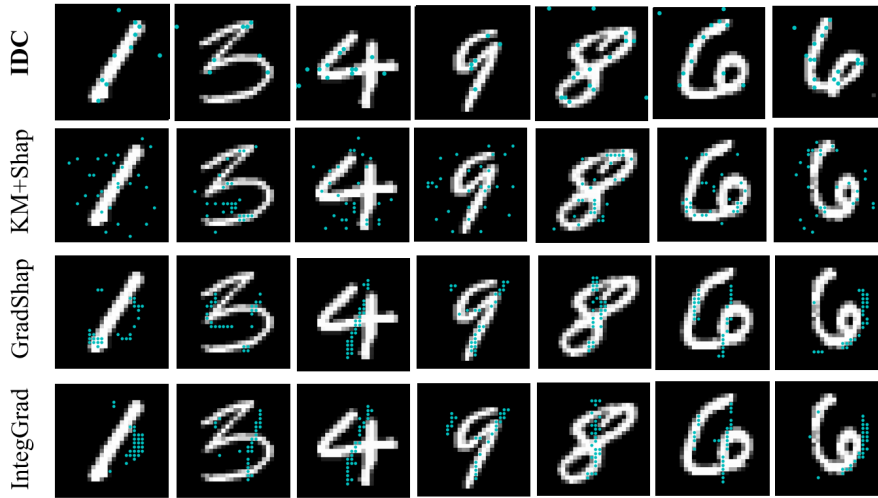


Figure 4: Features selected by different explainers on MNIST 10K subset: features learned during clustering training as proposed by our approach (top), features selected by Shap explainer with KMeans predictor (KM-Shap), features obtained from the Gradient-Shap explainer with trained clustering model (GradShap) and features predicted by Integrated Gradients explainer (bottom).

samples that are used as a background during Shap training, we select additional 100 random MNIST images that are not in the train set. Once the Shap model is trained, we take 15 top feature importance indices, the number of selected gates by our model. The intuition behind that is the desire to explain the clustering model with minimal features to stay useful for practitioners. As indicated in Table 2, our method produces more expressive features as sample-level explanations with the highest uniqueness score. In addition, our model outperforms Shap in faithfulness, as presented in Figure 3. It is easy to see that the accuracy drop correlates with feature importance. Additionally, Figure 4 presents the active gates selected for each sample. It can be seen that **IDC** selects more informative features which are local for each sample.

### 6.4.3 Clustering MNIST and FashionMNIST benchmarks

In this experiment, we train two versions of our model for each dataset. The first version learns clustering assignments without local gates, so the autoencoder is fed raw input samples with  $D = 784$ . The second version is our full model with a gating network that reduces the number of non-zero gates to the minimum. Both models are trained on 60,000 dataset samples with the same hyperparameters.

Table 4: Clustering Accuracy, Adjusted Rand Index, Normalized Mutual Information, and the number of features selected by using our method on MNIST and FashionMNIST datasets. The proposed model improves clustering accuracy by using only about 16 features out of 784 on MNIST and about 69 features on FashionMNIST datasets.

Dataset	Method	ACC	ARI	NMI	$ S $
MNIST	IDC (w/o gates)	81.1 $\pm$ 0.08	75.9 $\pm$ 0.07	<b>80.3</b> $\pm$ 0.04	784
	IDC	<b>84.3</b> $\pm$ 0.08	<b>76.9</b> $\pm$ 0.07	79.7 $\pm$ 0.04	<b>15.81</b> $\pm$ 0.23
FashionMNIST	IDC (w/o gates)	61.0 $\pm$ 0.03	<b>49.3</b> $\pm$ 0.03	62.7 $\pm$ 0.02	784
	IDC	<b>61.9</b> $\pm$ 0.04	49.1 $\pm$ 0.02	<b>63.3</b> $\pm$ 0.01	<b>68.6</b> $\pm$ <b>0.20</b>

Table 5: Clustering Accuracy on Real Datasets.  $K$ -Means accuracy is borrowed from [19].  $|S|$  is calculated by taking the median on a batch of gates produced by LSTG and the mean value across ten experiments.

Method / Dataset	TOX-171	ALLAML	PROSTATE	SRBCT	BIASE	INTESTINE
KMeans (D)	41.5 $\pm$ .02	67.3 $\pm$ .03	58.1 $\pm$ .00	39.6 $\pm$ .03	41.8 $\pm$ .08	54.8 $\pm$ .03
LS+KM	47.5 $\pm$ .01	73.2 $\pm$ .00	58.6 $\pm$ .00	41.1 $\pm$ .03	83.8 $\pm$ .00	43.2 $\pm$ .03
MCFS+KM	42.5 $\pm$ .03	72.9 $\pm$ .02	57.3 $\pm$ .00	43.7 $\pm$ .03	95.5 $\pm$ .03	48.2 $\pm$ .04
SRCFS+KM	45.8 $\pm$ .06	67.7 $\pm$ .06	60.6 $\pm$ .02	33.5 $\pm$ .05	50.8 $\pm$ .05	58.1 $\pm$ .10
CAE+KM	47.7 $\pm$ .01	73.5 $\pm$ .00	56.9 $\pm$ .00	<b>62.6</b> $\pm$ .07	85.1 $\pm$ .02	51.9 $\pm$ .03
DUFS+KM	49.1 $\pm$ .03	<b>74.5</b> $\pm$ .01	64.7 $\pm$ .00	51.7 $\pm$ .01	<b>100</b> $\pm$ .00	71.9 $\pm$ .07
<b>IDC</b>	<b>50.6</b> $\pm$ .03	72.2 $\pm$ .03	<b>65.3</b> $\pm$ .03	55.4 $\pm$ .05	95.7 $\pm$ .01	<b>74.2</b> $\pm$ .02
$ S $	49.6 $\pm$ 8.7	307.6 $\pm$ 2.5	170.9 $\pm$ 2.96	46.7 $\pm$ 2.20	210 $\pm$ 0.00	65 $\pm$ 0.0
D / N / K	5748 / 171 / 4	7192 / 72 / 2	5966 / 102 / 2	2308 / 83 / 4	25683 / 56 / 4	3775 / 238 / 13

The Encoder consists of 4 linear layers with batch normalization and ReLu non-linearity with hidden layers of sizes [512, 512, 2048, 10]. The Decoder has the same but reversed structure. In addition, the clustering head has a single hidden layer of size 2048.

Table 4 demonstrates how the gating network contributes to accurate clustering and selects a small subset of features.

#### 6.4.4 Real world data

This section evaluates our method using six real tabular datasets commonly used for evaluating feature selection schemes. The datasets are collected from different biological domains and often contain more features than samples. Such a regime of high dimensions and a low sample size is highly challenging for unsupervised clustering models. Specifically, standard clustering models fail to model the cluster assignments accurately. Table 5 presents clustering accuracy of different methods:  $K$ -Means<sup>4</sup> on the full set of features, (KMeans(D)), SRCFS feature selector [9] with  $K$ -Means (SRCFS+KM), Concrete Autoencoders feature selector with  $K$ -Means clustering on the selected features (CAE+KM) [1], DUFS feature selector [19] with  $K$ -Means clustering (DUFS+KM), our model where the best checkpoint chosen by Silhouette score and our best model in terms of accuracy. In addition, we present the number of selected features for each dataset by our model ( $|S| \leq D$ ). Our model produces comparable clustering accuracy to the feature selection methods integrated with  $K$ -means and even outperforms them on 3 datasets.

## 7 Conclusions

We proposed a deep clustering model that produces accurate cluster assignments and predicts the informative feature set for interpretability. The model was evaluated on diverse datasets: a synthetic dataset, commonly used deep clustering image benchmarks, and high-dimensional low sample size bio-med tabular datasets. The gating network enables built-in interpretability of our model such that the clustering is done on the sparse input but is still informative for the task. There is still an open research direction on the best clustering architectures that could be integrated into the proposed model: should the clustering subnetwork be simplified to depend more on selected gates rather than on clustering objective function. We hope our work will benefit scientists in the bio-med domain.

<sup>4</sup>Implemented here: <https://scikit-learn.org/stable/modules/generated/sklearn.cluster.KMeans.html>

## References

- [1] A. Abid, M. F. Balin, and J. Zou. Concrete autoencoders for differentiable feature selection and reconstruction. *arXiv preprint arXiv:1901.09346*, 2019.
- [2] D. Alvarez Melis and T. Jaakkola. Towards robust interpretability with self-explaining neural networks. *Advances in neural information processing systems*, 31, 2018.
- [3] Y. Bregman, O. Lindenbaum, and N. Rabin. Array based earthquakes-explosion discrimination using diffusion maps. *Pure and Applied Geophysics*, 178:2403–2418, 2021.
- [4] J. Cai, J. Fan, W. Guo, S. Wang, Y. Zhang, and Z. Zhang. Efficient deep embedded subspace clustering. In *Proceedings of the IEEE/CVF Conference on Computer Vision and Pattern Recognition*, pages 1–10, 2022.
- [5] S. F. Farhadian, O. Lindenbaum, J. Zhao, M. J. Corley, Y. Im, H. Walsh, A. Vecchio, R. Garcia-Milian, J. Chiarella, M. Chintanaphol, et al. Hiv viral transcription and immune perturbations in the cns of people with hiv despite art. *JCI insight*, 7(13), 2022.
- [6] N. Frost, M. Moshkovitz, and C. Rashtchian. Exkmc: Expanding explainable  $k$ -means clustering. *arXiv preprint arXiv:2006.02399*, 2020.
- [7] B. Gao, Y. Yang, H. Gouk, and T. M. Hospedales. Deep clustering with concrete k-means. In *Icassp 2020-2020 IEEE International Conference on Acoustics, Speech and Signal Processing (ICASSP)*, pages 4252–4256. IEEE, 2020.
- [8] Y. Guan, M. I. Jordan, and J. G. Dy. A unified probabilistic model for global and local unsupervised feature selection. In *Proceedings of the 28th International Conference on Machine Learning (ICML-11)*, pages 1073–1080, 2011.
- [9] D. Huang, X. Cai, and C.-D. Wang. Unsupervised feature selection with multi-subspace randomization and collaboration. *Knowledge-Based Systems*, 182:104856, 2019.
- [10] S. Jana, H. Li, Y. Yamada, and O. Lindenbaum. Support recovery with stochastic gates: Theory and application for linear models. *arXiv preprint arXiv:2110.15960*, 2021.
- [11] E. Jang, S. Gu, and B. Poole. Categorical reparameterization with gumbel-softmax. *arXiv preprint arXiv:1611.01144*, 2016.
- [12] V. Y. Kiselev, K. Kirschner, M. T. Schaub, T. Andrews, A. Yiu, T. Chandra, K. N. Natarajan, W. Reik, M. Barahona, A. R. Green, et al. Sc3: consensus clustering of single-cell rna-seq data. *Nature methods*, 14(5):483–486, 2017.
- [13] C. Lee, F. Imrie, and M. van der Schaar. Self-supervision enhanced feature selection with correlated gates. In *International Conference on Learning Representations*, 2022.
- [14] Z. Li, Y. Chen, Y. LeCun, and F. T. Sommer. Neural manifold clustering and embedding. *arXiv preprint arXiv:2201.10000*, 2022.
- [15] O. Lindenbaum, M. Salhov, A. Averbuch, and Y. Kluger. L0-sparse canonical correlation analysis. In *International Conference on Learning Representations*.
- [16] O. Lindenbaum, N. Rabin, Y. Bregman, and A. Averbuch. Multi-channel fusion for seismic event detection and classification. In *2016 IEEE International Conference on the Science of Electrical Engineering (ICSEE)*, pages 1–5. IEEE, 2016.
- [17] O. Lindenbaum, Y. Aizenbud, and Y. Kluger. Probabilistic robust autoencoders for outlier detection. *arXiv preprint arXiv:2110.00494*, 2021.
- [18] O. Lindenbaum, N. Nouri, Y. Kluger, and S. H. Kleinstejn. Alignment free identification of clones in b cell receptor repertoires. *Nucleic acids research*, 49(4):e21–e21, 2021.
- [19] O. Lindenbaum, U. Shaham, E. Peterfreund, J. Svirsky, N. Casey, and Y. Kluger. Differentiable unsupervised feature selection based on a gated laplacian. *Advances in Neural Information Processing Systems*, 34:1530–1542, 2021.

- [20] S. M. Lundberg and S.-I. Lee. A unified approach to interpreting model predictions. *Advances in neural information processing systems*, 30, 2017.
- [21] J. Lv, Z. Kang, X. Lu, and Z. Xu. Pseudo-supervised deep subspace clustering. *IEEE Transactions on Image Processing*, 30:5252–5263, 2021.
- [22] V. Mikuni and F. Canelli. Unsupervised clustering for collider physics. *Physical Review D*, 103(9):092007, 2021.
- [23] C. Niu, H. Shan, and G. Wang. Spice: Semantic pseudo-labeling for image clustering. *arXiv preprint arXiv:2103.09382*, 2021.
- [24] C. K. Reddy, M. Al Hasan, and M. J. Zaki. Clustering biological data. *Data Clustering*, pages 381–414, 2018.
- [25] F. Reverter, E. Vegas, and J. M. Oller. Kernel-pca data integration with enhanced interpretability. *BMC systems biology*, 8(2):1–9, 2014.
- [26] A. Rozner, B. Battash, L. Wolf, and O. Lindenbaum. Domain-generalizable multiple-domain clustering. *arXiv preprint arXiv:2301.13530*, 2023.
- [27] U. Shaham, K. Stanton, H. Li, B. Nadler, R. Basri, and Y. Kluger. Spectralnet: Spectral clustering using deep neural networks. *arXiv preprint arXiv:1801.01587*, 2018.
- [28] U. Shaham, O. Lindenbaum, J. Svirsky, and Y. Kluger. Deep unsupervised feature selection by discarding nuisance and correlated features. *Neural Networks*, 152:34–43, 2022.
- [29] Y. Shen, Z. Shen, M. Wang, J. Qin, P. Torr, and L. Shao. You never cluster alone. *Advances in Neural Information Processing Systems*, 34:27734–27746, 2021.
- [30] G. Sokar, Z. Atashgahi, M. Pechenizkiy, and D. C. Mocanu. Where to pay attention in sparse training for feature selection? *arXiv preprint arXiv:2211.14627*, 2022.
- [31] M. Sundararajan, A. Taly, and Q. Yan. Axiomatic attribution for deep networks. In *International conference on machine learning*, pages 3319–3328. PMLR, 2017.
- [32] B. M. Varghese, A. Unnikrishnan, G. Scientist, N. Kochi, and C. Kochi. Clustering student data to characterize performance patterns. *Int. J. Adv. Comput. Sci. Appl*, 2:138–140, 2010.
- [33] Y. Yamada, O. Lindenbaum, S. Negahban, and Y. Kluger. Feature selection using stochastic gates. In *International Conference on Machine Learning*, pages 10648–10659. PMLR, 2020.
- [34] J. Yang, O. Lindenbaum, and Y. Kluger. Locally sparse neural networks for tabular biomedical data. In *International Conference on Machine Learning*, pages 25123–25153. PMLR, 2022.
- [35] J. Yoon, J. Jordon, and M. van der Schaar. Invase: Instance-wise variable selection using neural networks. In *International Conference on Learning Representations*, 2019.
- [36] Y. Yu, K. H. R. Chan, C. You, C. Song, and Y. Ma. Learning diverse and discriminative representations via the principle of maximal coding rate reduction. *Advances in Neural Information Processing Systems*, 33:9422–9434, 2020.

## A Model architecture

We report the model architecture for different datasets. All datasets are trained with the single hidden layer in the ClusterHead and GatingNet.

Table 6: The architectures of the model for different datasets. The first value in the Encoder list is the input dimension, while the last value is the Autoencoder latent embedding dimension which is shared between Encoder and Decoder. The last value in the ClusterHead is the number of categories. GatingNet encodes the input into the same dimension.

Dataset	Encoder	Decoder	ClusterHead	GatingNet
Synthetic	[13, 10, 8]	[8, 10, 13]	[8, 2, 4]	[13, 16, 13]
MNIST	[784, 512, 512, 2048, 10]	[10, 2048, 512, 512, 784]	[10, 2048, 10]	[784, 784, 784]
FashionMNIST	[784, 512, 512, 2048, 10]	[10, 2048, 512, 512, 784]	[10, 2048, 10]	[784, 784, 784]
TOX-171	[5748, 512, 256, 128]	[128, 256, 512, 5748]	[128, 32, 4]	[5748, 32, 5748]
ALLAML	[7129, 128, 64]	[64, 128, 7129]	[64, 8, 2]	[7129, 32, 7129]
PROSTATE	[5966, 256, 128, 128]	[128, 128, 256, 5966]	[128, 32, 2]	[5966, 32, 5966]
SRBCT	[2308, 256, 128, 128]	[128, 128, 256, 2308]	[128, 32, 4]	[2308, 32, 2308]
BIASE	[21810, 128, 512, 256, 128]	[128, 256, 512, 128, 21810]	[128, 32, 4]	[21810, 64, 21810]
INTESTINE	[3775, 1024, 512, 256, 128]	[128, 256, 512, 1024, 3775]	[128, 32, 13]	[3775, 32, 3775]

## B Training Setup

We train all models with a two-stage approach - we train Encoder, Decoder, and GatingNet in the first stage and then train ClusterHead in the second stage. We use Adam optimizer for modules (Encoder, Decoder, GatingNet) with a learning rate of  $1e - 3$  and a learning rate of  $1e - 2$  for the ClusterHead. To train global gates matrix with use SGD optimizer with learning rate  $1e - 1$ .

Table 7: The number of epochs and batch size for different datasets.

Dataset	Epochs Stage 1	Epochs Stage 2	Batch size
Synthetic	50	2000	800
MNIST	100	600	256
FashionMNIST	100	500	256
TOX-171	10000	2000	171
ALLAML	10000	1000	72
PROSTATE	10000	1000	102
SRBCT	2000	1000	83
BIASE	2000	4000	301
INTESTINE	4000	2000	238

## C Maximum Coding Rate Modification

For simplicity in the presentation of our work, we slightly modify the original formula of the Coding Reduction Rate. As presented in the paper we use the next formula for the gating network optimization:

$$\mathcal{L}_{gtr} = -\frac{1}{2} \cdot \log\det(\mathbf{I} + \lambda_1 \cdot \mathbf{Z}\mathbf{Z}^T), \quad (9)$$

where is defined by  $\lambda_1 = d_{input} \cdot (B * \epsilon)$ , where  $\epsilon$  is the the coding error hyper parameter,  $B$  is a batch size and  $d_{input}$  is the dimension of the input sample. Similarly, for the clustering loss term represented by:

$$\mathcal{L}_{head} = \sum_{k=1}^K \frac{1}{2} \cdot \log\det(\mathbf{I} + \lambda_2 \cdot \mathbf{H}_k \mathbf{H}_k^T), \quad (10)$$

we use  $\lambda_2 = d_{emb} \cdot (B * \epsilon)$  where the  $d_{emb}$  is the dimension of the embedding vector for each sample. We use the same  $\epsilon$  for both loss terms in our experiments.

## **D Strengths and Limitations**

The proposed model was tested on low sample size datasets and two commonly used benchmarks in deep clustering. The model achieves comparable clustering results in terms of accuracy and provides sample-level and cluster-level interpretability.

The design of the model architecture remains dataset-specific. In addition, we applied a manual search for the best hyperparameters for each dataset. In spite of that, the main requirement for good clustering in the proposed approach is to train a good autoencoder for reconstruction where the reconstruction loss serves as a label-independent metric for hyperparameter tuning. In addition, it is an open question if the clustering head should include more parameters or only a single linear projection from the learned gated input representation. We plan in the future to test additional model architectures and clustering objective functions.